Evaluation of Fracture Toughness of Welded High Strength Low Alloy Line-pipe Steel

Banda Venkata Bhargava

Department of Metallurgical and Materials Engineering

National Institute of Technology Rourkela

Evaluation of fracture toughness of welded high strength low alloy line-pipe steel

Thesis submitted to the

National Institute of Technology Rourkela

in partial fulfillment of the requirements

of the degree of

Master of technology

in

Metallurgical and Materials Engineering

by

Banda Venkata Bhargava

(Roll Number: 214MM1337)

Under the supervision of

Prof. Krishna Dutta
and
Dr. Shrabani Majumdar

May 2016

Department of Metallurgical and Materials Engineering
National Institute of Technology Rourkela

Metallurgical and Materials Engineering

National Institute of Technology Rourkela

Dr. Krishna Dutta
Assistant Professor
Metallurgical and Materials Engineering
NIT Rourkela

May 26, 2016

Supervisor's Certificate

This is to certify that the work presented in this thesis entitled *"Evaluation of Fracture toughness of Welded High Strength Line-pipe Steel*" by "*Banda Venkata Bhargava*", Roll Number 214MM1337, is a record of original research carried out by him under my supervision and guidance in partial fulfillment of the requirements of the degree of *Masters in Technology* in *Metallurgical and Materials Engineering*. Neither this thesis nor any part of it has been submitted for any degree or diploma to any institute or university in India or abroad.

Krishna Dutta
Principal Supervisor

Material Characterization and Joining Group

R & D, TATA Steel Ltd. Jamshedpur

Dr. Shrabani Majumdar
Principal Scientist
Material Characterization and Joining Group
R & D, TATA Steel Ltd
Jamshedpur

May 26, 2016

Co-Supervisor's Certificate

This is to certify that the work presented in this thesis entitled *"Evaluation of Fracture Toughness of Welded High Strength Line-pipe Steel*" by "*Banda Venkata Bhargava*", Roll Number 214MM1337, is a record of original research carried out by him under our supervision and guidance in partial fulfillment of the requirements of the degree of Masters of Technology in *Metallurgical and Materials Engineering*. Neither this thesis nor any part of it has been submitted for any degree or diploma to any institute or university in India or abroad.

Shrabani Majumdar
Co-Supervisor

Dedicated

To

My

Parents and Friends

Declaration of Originality

I, Banda Venkata Bhargava, Roll Number *214MM1337* hereby declare that this thesis entitled "*Evaluation of Fracture Toughness of Welded High Strength Line-pipe Steel*" represents my original work carried out as a postgraduate student of NIT Rourkela and, to the best of my knowledge, it contains no material previously published or written by another person, nor any material presented for the award of any other degree or diploma of NIT Rourkela or any other institution. Any contribution made to this research by others, with whom I have worked at NIT Rourkela or elsewhere, is explicitly acknowledged in the thesis. Works of other authors cited in this thesis have been duly acknowledged under the section "Bibliography". I have also submitted my original research records to the scrutiny committee for evaluation of my thesis.

I am fully aware that in case of any non-compliance detected in future, the Senate of NIT Rourkela may withdraw the degree awarded to me on the basis of the present thesis.

May 26, 2016 *Banda Venkata Bhargava*

NIT Rourkela

Acknowledgment

The satisfaction and euphoria that accompany the successful completion of a task would be incomplete without the mention of the people who made it possible and whose constant guidance and encouragement crowned all the efforts with success.

Therefore, I would like to take this opportunity to express my sincere and heartfelt gratitude to all those who made this report possible.

At first I would like to thank my Guide, Thesis supervisor **Prof. Krishna Dutta** Department of Metallurgical & Materials Engineering, National Institute of Technology, Rourkela who permits me to work at Research and Development, Scientific Services, Tata Steel, Jamshedpur. Without his support and invaluable guidance, it is impossible for me to complete this work.

I bow humbly to record my deep sense of gratitude to my Co-Supervisor **Dr. Shrabani Majumdar** Principle Scientist, Research and Development, Scientific Services, Tata Steel Ltd, Jamshedpur, who always motivate me and enlighten me with her valuable suggestions. With her constant encouragement and able guidance during every stage of the work that brought the research to a successful completion.

I thank **Prof. S. C. Misra** Head of the Department Metallurgical and Materials Engineering, National Institute of Technology, Rourkela, who has encouraged a lot to carry out this project work at Tata Steel.

I am also grateful to **Dr. Kanwer Singh Arora, Tata Steel Ltd**, Jamshedpur, for encouraging, providing research facilities, helping me in analyzing data and supporting during this investigation.

I thank my beloved friends of various colleges worked along with me in Tata Steel Ltd Jamshedpur **Mr. Govardhan Pujari, Mr. Rajath Rautela, Mr. Pramay Bhatprahari, Mr. Aditya Arun** and **Mr. Shaswath Sharma**, who made my stay colorful.

At last but not the least I thank my **Parents and Family Members** without whom support and motivation I couldn't complete this work.

May 26, 2016 — *Banda Venkata Bhargava*

NIT Rourkela — (Roll Number: 214MM1337)

Abstract

The present investigation revolves around evaluation of fracture toughness of welded API X65 steel plate. API X65 is a high strength low alloy (HSLA) steel which is used in line-pipes for transporting oil and natural gas. In the above application, catastrophic failure due to fatigue is reported to cause sudden damage and loss to human-life as well as property. Hence, from end application point of view, knowledge on fracture toughness especially in welded plates is of immense importance. Through the present work, an effort has been made to add to the limited number of reports on the above subject. In this work, first, the selected steel was characterized in terms microstructure, hardness and tensile properties. Thereafter, the welding of steel plates was performed with sub merged arc welding (SAW) with root pass of shielded metal arc welding (SMAW). The microhardness profile in base material (BM), heat affected zone (HAZ), weld zone (WZ) and weld nugget were evaluated along with microstructural characterization of the above zones using optical and transmission-electron microscopy. The fracture toughness of various zones of welded plate, was evaluated in terms of J-R curve following the concept of EPFM. The samples for fracture toughness tests were prepared as per ASTM E1820. Fractography of the failed specimens were also carried out. The evaluation of fracture toughness of welded API X65 plates indicates that, J_Q value of heat affected zone was slightly lower than the base material, but for the weld zone it dropped significantly by 53% due to the non-uniform crack front and crack propagation. The phenomenon is attributed to presence of different defects in the weld region. J_Q value for fusion line samples showed significant scatter with an average reduction of 40% in J_Q value as compared to base material. The scatter in fusion line value can be attributed to error in precise placement of notch or deviation of crack path during testing. Presence of Nb and V imparts precipitation hardening effect to the API X65 steel, such that it has a satisfactory combination of strength and toughness parameters fulfilled by API service requirements.

Keywords: Sub merged arc welding (SAW); Shielded metal arc welding (SMAW); Base material (BM); Heat affected zone (HAZ); Weld zone (WZ); Fracture toughness

Contents

List of figures

List of tables

Chapter 1

Introduction

1.1 Background and motivation

Over the past few years, production of oil and gas increased enormously and due to this, the transport of such oils and gasses require development of improved line-pipe steels. The usage of high strength low alloy steels (HSLA) in line-pipe brings in the advantage of cost reduction by virtue of reduction in wall thickness of pipelines [1]. Manufacturing of HSLA line-pipe steel for oil and gas transmission follows the API 5L standard [2]. The desired properties in these steels are high mechanical strength, good weldability, high fracture toughness, strain tolerance, resistance to environmental degradation such as stress corrosion cracking. The aim of steel suppliers is to develop all the above properties at a reasonable price. These steels were first introduced in early 1930`s which was followed by years of research to achieve optimum structure-property combination. The micro-alloying elements like niobium, vanadium and titanium were added in certain amounts as low as 0.005-0.010 percent in early steels. These HSLA steels were firstly used in ship plates, beams, bridge steels, reinforcing bar and heat treated forgings and was not introduced into line-pipe steels until 1959 [3]. However due to the predominant changes in the metallurgical approaches and development of different kinds of rolling techniques these HSLA steels came into existence with the escalating technological demands of high pressure line-pipe steel.

In this work, a special grade of HSLA steel developed at TATA steel Ltd., Jamshedpur, India, was characterised. It was specially aimed to develop a suitable combination of strength and toughness for the steel owing to different microalloying additions. The study also compares the properties of the steel and its weldments.

1.2 Objectives of the current work

The primary objective of the present investigation is to study and evaluate the fracture toughness of the welded high strength line-pipe steel. The major scope of the work is briefly summarised as follows:

(I) To characterize the steel for its chemical composition, its microstructure in base metal and weld regions and to determine the hardness and tensile properties.

This section consists of (a) chemical composition analysis of the steel specimens (b) microstructural examination at various zones i.e. parent material, heat affected zone, weld zone and grain size measurement (c) determination of their hardness and tensile properties.

(II) To study the facture toughness property of the welded API X65 steel.

The major experiments to fulfil this objective are (a) pre-cracking of the sample under fatigue (b) examination of the fracture toughness at various zones by J-R curve approach.

(III) Fractographic examinations on the fractured sample using (SEM) scanning electron microscope.

Fractographic examinations of fractured surface using SEM to study the various features and understand the type of failure in the fractured sample.

Chapter 2

Literature Review

2.1 Introduction

High-strength low-alloy steel (HSLA) were firstly introduced in early 1930`s. The elements like niobium vanadium and titanium were added independently in amounts of about 0.005 to 0.010 in early steels, however as strength increased with adding them in combination and the metallurgical approaches got more refined. The overriding melting method at early days was Siemens- Martin open hearth process, the steels were ingot usually semi-killed, and in many cases were normalized. And due to the drastic change in the manufacturing processes very low carbon fully killed steels, were continuously casted and brought to the required shape by the use of Thermomechanical controlled process (TMCP). HSLA steels were firstly used in the ship construction, bridges, reinforced bars but not introduced into line-pipe application until 1959 [3]. Then after the boom in the technology has brought to the application into line-pipe steel with rapid evolution of HSLA technology since then. HSLA is a type of alloy steel that provides very good mechanical properties and are very highly resistant to corrosion than carbon steel. HSLA steels are different from other steels that these are not made to meet the specific chemical composition, however to meet the specific mechanical properties depending on the application by varying the micro alloying elements accordingly. These steels will have a very less carbon content varying from 0.05 to 0.025% to respond easily during forming and welding operations. Other alloying elements are added approximately up to 2.0% manganese and very little amounts of copper, niobium, nickel, vanadium, titanium, chromium, nitrogen, molybdenum or zirconium [4, 5]. Cu, Ti, V and Nb are added for strengthening purposes [5]. These elements are deliberately added to alter the microstructure of carbon steels, which is generally the amalgamation of

ferrite-pearlite, to produce a very fine scattering of alloy carbides in an almost pure ferrite matrix [6].

Mostly used in cars, cranes, trucks, bridges and other structures where huge amounts of stress has to be handled and excellent strength to weight ratio is required. However, these steels are good at strength to weight ratio their cross sections and structures are lighter by 20 to 30% compared to carbon steels with same strength [6].

HSLA steels are more resistant to corrosion than most carbon steels due to lack of pearlite – and fine layers of ferrite (almost pure iron) and cementite in pearlite. HSLA steels usually have densities of around 7800 kg/m³ [7].

2.2 Classification of HSLA steel

HSLA steels include many standard grades covered by ASTM standards designed to provide particular strength, toughness, formability, weldability, and to with stand from corrosion depending on the application of the material. HSLA steels are not the alloy steels even though some amount of alloying elements are added to the steels to meet the requirement. Particularly these are separate steels which are similar to as-rolled carbon steels with improved mechanical properties by adding the alloying elements, and special rolling techniques such as controlled rolling and rapid cooling techniques which are explained briefly later. Because of this they are priced at the base price of carbon steels not at the base price of the alloy steels which will be a bit expensive compared to the carbon steels. However these steels are sold with minimum mechanical properties with the specific alloy content left to the discretion to the steel producers. These steels are classified into six categories [8, 9] weathering steels, microalloyed steels, rolled pearlitic steels, acicular ferrite steels, dual phase steels, inclusion-shape-controlled-steels.

2.3 Effects of alloying elements

Manganese is one of the vital element in the line-pipe steels which plays a major role because it will merges with Sulphur to form MnS. Which will cause hot shortness in steels. Therefore, the addition of manganese with Sulphur and formation will vulnerable of a steel to hot shortness [10]. It is added to steels to not only improve the hot working

properties of the steel, but it also improves the strength, toughness, hardenability. Iron sulphide has lower melting point than MnS, which tends to form at the austenite boundaries in the absence of manganese there are chances of increase in potential crack growth sites during hot working [11]. With little amount of carbon with high amount of manganese (Mn 0.8-0.15%) in steel design is depends on manganese leads to solid solution strengthening [11].Silicon is one of the deoxidizer used in steel making. Silicon exhibits properties like increase of solid solution hardening effect on ferrite and used to improve the strength and toughness [10]. The strengthening rate of low carbon steels by Si was higher in coarse grain region compared to that of the fine grain region. But, silicon decreases the prior austenite grain size which leads to a fine ferrite grain size [12]. Increasing the amount of silicon will results in decrease in the rate of recrystallization and increase the strength of austenite due to the solid solution hardening [13].Molybdenum also has a great effect on increasing the high temperature strength and retarding grain growth at temperatures just above the critical temperatures of steel [10]. It increases the steel hardenability and shows very good resistance to hydrogen embrittlement and stress corrosion cracking in high Sulphur content steels [14]. It has also been reported that adding molybdenum to Microalloyed steels results in the slowing down of the bainitic transformation which results in a fine bainitic region [15]. It is the most important element in the micro alloying elements to stabilize the carbon and has very adverse effect on austenite recrystallization and hardenability [10]. The rate of initial transformation of austenite to high ferrite niobium steels is reduced by the solute drag effect of niobium and pinning effect of the Nb(CN) precipitates [16].Vanadium is used to interfere the austenite grain growth at peak temperatures results in fine grain therefore achieves good toughness and strength [10]. But, steels that are hardened by precipitation hardening with vanadium carbide exhibits poor wear resistance than vanadium free steels. Vanadium and Silicon has a vital role in the microstructure and hardness. Microalloying with Titanium results in the deceleration of austenite recrystallization along with precipitation strengthening of ferrite. Titanium amalgamates with carbon and forms titanium carbides, which are highly stable and difficult to dissolve in austenite. Titanium subsequently improves the weldability and resistant to HAZ cold cracking due to TiC precipitate particles which acts as the effective traps for hydrogen atoms [17].

Chromium is added to increase the corrosion resistance of the steels. It also increases the hardenability and wear resistance of the steels. Chromium amount more than 4 weight % in steels increases the corrosion resistance. However there will be a subsequent decrease in the weldability. Chromium can form Cr_3C_2 by this the wear resistance increases enormously [10]. Chromium polarizes the cathodic polarization curves of line-pipe steels which helps in uneven corrosion rate in the line-pipe weldments [18]. Nickle improves oxidation and corrosion properties of steels along with this it also improves toughness, impact resistance and solid solution strengthening. Nickle also helps in forming of very finer pearlite as pearlite is very strong and tougher results in very high toughness and has no adverse effect on welding [10]. Aluminium is added as a deoxidizer to steels. But adding this in excessive amount will results in decrease in toughness and the deoxidizing function ends i.e. at weight% greater than 0.05. Aluminium likely to form aluminium nitride (AlN) which has a very severe effect on hot ductility of different grades. If weight % of aluminium increases by 0.02 it promotes precipitation of AlN rather than vanadium nitride [21]. Copper is regarded as the dangerous element as it causes hot shortness which reduces ductility of the material at temperatures 1100~1300^{o}C. It also causes surface defects during hot processing and it has been reported [20]. But, it increases the corrosion resistance and tensile properties of steels. It is usually the element which causes embrittlement in low alloy steels. Which promotes grain boundaries to segregate and reduces the toughness property. It increases the tendency to cracking while welding because of the embrittlement property present in it so due to this reason the amount of phosphorous should be low as 0.015 weight% [21]. But when it is present in phosphate form it reduces the hydrogen uptake. Sulphur is a harmful element in steels which form sulphide inclusion with manganese and reduces the toughness properties in steels. Sulphur will separate the grain boundaries which causes intergranular fracture [11]. Nitrogen it has been considered as one of the vital and low cost alloying additions to steels. Nitrogen will be present in the interstitial atoms as nitrides of iron, titanium, vanadium, aluminium, niobium and other alloying elements. Depending upon the form it can be treated a s harmful or beneficial to physical and mechanical properties of the steels. Because it is a small atom like carbon can easily diffuses in the steels and causes surface hardening.

2.4 Processing and manufacturing of line-pipe steels

An important factor affecting strength and toughness of the material was rolling process involved in the manufacturing of HSLA steels they are:

1. Thermomechanical Controlled Rolling (TMCR)
2. Thermomechanical controlled process (TMCP)

The TMCR consists in rolling slabs into plates in three main steps.

- First, rolling in temperatures of austenite recrystallization (around 1250^{o}C),
- Second, rolling in austenite non-recrystallization temperatures (around 1050^{o}C),
- Third, finishing rolling in austenite – ferrite Ar3 temperature(910^{o}C) (or even at lower temperatures depending on the carbon content and on the mechanical resistance aimed)
- Finally air cooled.

The TMCP is similar to TMCR process for first three steps followed by accelerated cooling i.e. with water after the third step of the controlled rolling [22, 23].

However, there is a difference between both TMCR and TMCP processes, the final rolling pass temperature. In the TMCR process this temperature is lower because, as this process does not have accelerated cooling, the mechanical properties should be guaranteed during the final rolling pass. Reducing the temperature in this third step of the process TMCR gives the material micro textures in the steel microstructure. These textures have different orientations through steel plate's thicknesses, which causes the development of residual stresses in the as rolled material and which allows the appearance of separations.

2.5 HSLA steels applications

HSLA steels are widely used in automotive industry, in oil and gas industry where fluids or gases with very high pressure has to be transferred for huge distances, in earth movers

and heavy off road vehicles, industrial equipment, construction of bridges, trusses, storage tanks, power transmission lines, in civil constructions etc. these are the additional applications of this steels.

The choice of particular kind of steel depends on the application in which it is going to be used depending number of application requirements like thickness, corrosion resistant, formability, and weldability. Mostly in selection process of steels strength to weight ratio of HSLA compared with normal low carbon steels. This characteristics of HSLA leads to the application of line-pipes also [8].

2.5.1 HSLA steels in line-pipe applications

HSLA techniques in line-pipe steels was firstly used in Mannesmann, Europe in normalized API Grade X-52 vanadium grades around 1952. Then later in 1953and 1962 further extended to API Grade X-56 and X-60 [24, 25].

Then in North America in the year 1959 hot rolled steel utilizing HSLA concepts came up into existence [3] and this replaced the normalising process completely in Europe by 1972 [24, 25, 26].

HSLA steel was still used in Europe till the mid 1990's and the applications and research work on this different kinds on API 5L grades is going on till date.

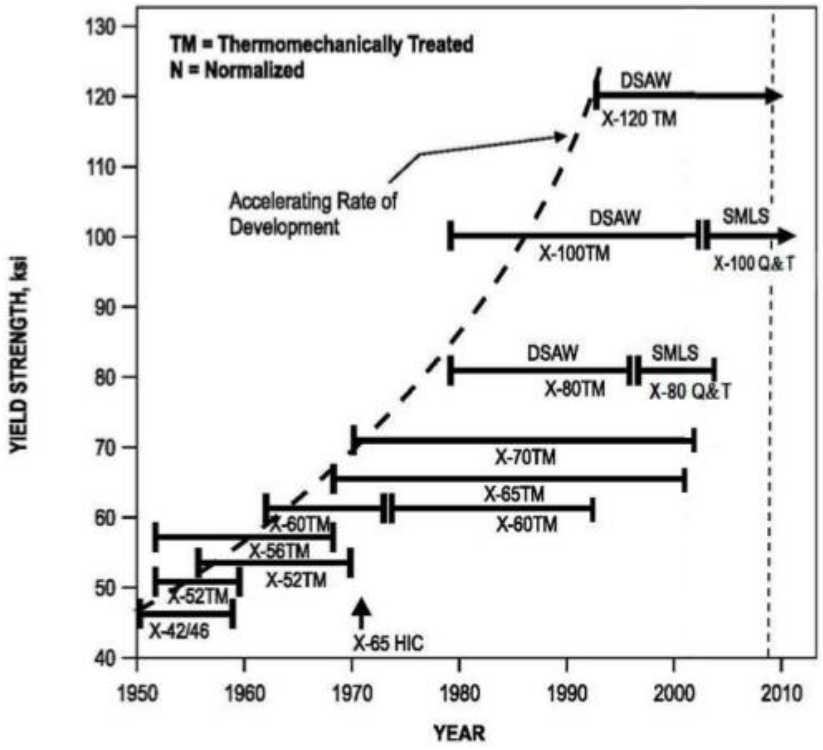

Figure 2.1: Evolution of line-pipe grade steel [26]

2.6 Literature on shielded metal arc welding (SMAW) and fracture toughness of HSLA steels

HSLA steels are welded because they are used in most practical applications. However conventional arc welding causes many detrimental effects on the TMCP microstructures and morphology variations. Changes in microstructure occurs when metal melts and resolidifies as a coarse grain cast microstructure. These conventional arc welding was firstly patented in 1892 by C.L Coffin of Detroit [27] for this welding process using a consumable metal electrode. This was the first recorded process by which metal melts from an electrode due to presence of arc to retain filler metal which adds alloying elements to the weld nugget. Due to this filler metal some adverse effects may alleviate in the weld nugget, however there will be no change in the heat affected zone (HAZ) because melting and solidification does not happened in this zone. So the only way to alter the microstructural variation in HAZ is by controlling the thermal cycle during

welding. Therefore great amount of research has been carried out in enhancing fracture toughness of heat affected zone in conventional arc welding process [28]. In literature it was reported by reducing the grain size of martensite-austenite constituents improve fracture toughness [29]. Upper bainite has found to have brittle phase with low fracture toughness. Low fracture toughness was not only because of upper bainite but there was a partial contribution of lath carbide distribution in microstructure this was reported by Johnson et al. [30]. The HAZ microstructure and properties can be controlled by varying heat input, toughness can be increased by the formation of lower bainite at lower heat inputs [31]. In spite of research efforts, arc welding leads to deterioration in base metal properties.

2.7 Literature on submerged arc welding (SAW) and fracture toughness of HSLA steels

Submerged arc welding (SAW) is a very economical process as compared to shielded metal arc welding (SMAW) process with high deposition rate of four to ten times more than that of SMAW with high heat inputs. As no visible arc`s and fumes are produced it is safe for workers in the vicinity of the equipment. Very high currents around 200-400A can be used without spatter because arc is completely shielded. Operator skill requirement is very minimal because travel speed and wire feed rate are controlled by the welding equipment itself. The sub merged arc welding process was first patented by Jones, Kennedy and Rothermund in the year 1935 [32]. Microstructural and properties of the weld metal are depended upon the chemical composition and the thermal cycle during welding. So higher deposition rates requires high heat inputs in SAW. Hence only chemical composition is available as a means of controlling the characteristics, like microstructural and toughness of the weld metal. Past studies states that acicular ferrite is the primary phase which plays vital role in improving the toughness in the weld materials [33]. These transformed products during welding forms randomly oriented short ferrite needle like structure with high angled grain boundaries. The fine grained and interlocked laths of acicular ferrite provides maximum resistance to cleavage fracture, which improves the notch toughness of the material. Hence it is suggested to increase the

acicular ferrite`s volume fraction in the weld metal by controlling the prior austenite grain size which can be achieved by adjusting alloy content in weld metal. Past investigations have reported that during transformation from austenite to ferrite, firstly ferrite is formed along the grain boundaries and thickens in perpendicular direction towards the plane of the austenite grain boundaries this grain boundary phase is termed as allotriomorph [34, 35]. It has been reported by liu et al. [36] that nucleation of acicular ferrite on oxide inclusions takes place in weld metals; which further increase the acicular ferrite phase and reduces the secondary phases which is recommended as acicular ferrite increases fracture toughness of the weld metal.

Research on fracture toughness of submerged arc welding in HSLA steels is very limited. Gosh et al. [37] reported variation in weld input parameters effect the tensile properties fracture and fracture toughness of the material due to the change in the morphology of weld consists of coarse and fine grains. He also reported that rise in the input energy declines the ultimate tensile strength, hardness but enhances the ductility of the weld. Lu et al. [38] reported that fracture toughness in base metal toughness will be always greater than that of weld region and HAZ because grain coarsening and spherical precipitates induced by welding heat input in WM and HAZ results a decrease in fracture toughness.

Volume fraction of acicular ferrite increases with increasing titanium content in submerged arc welded HSLA steels which has been reported by Beidokhti et al. [39] they have also reported that with increasing titanium content there was a phenomenal decrease in the MnS inclusions in the weld metal where Ti based inclusion increases impact toughness of the weld material. In further investigations proposed by Kiran et al. [40] they have reported that by increasing welding speed tend to degrade weld pool size leads to higher cooling rate that boost up the volume fraction of acicular ferrite phase and better weld bead mechanical properties.

2.8 Fracture toughness J calculation

The perfect evaluation of ductile fracture behavior is critical task in reliability assessment in line-pipe steels. An important parameter in the vulnerability of line-pipe steels was hydrogen embrittlement. Plethora of research investigation were carried out on hydrogen embrittlement and most of the tests imitate the procedure in the presence of high pressure hydrogen. However these results are adequate in the safety point of view and directly fracture toughness properties to be determined instead of assuming with some other means. Fracture toughness tests are done with large samples in order to maintain the plain strain condition [41].

2.10 J-integral

J-Integral was firstly proposed by Rice [42] as an energy integral which can be used as distinct tool to find out the region under the elastic plastic conditions under crack tip stress and strain. During initial crack extension most of the steels shows considerable increase in the fracture toughness described by J-integral method commonly crack propagation was tested by TPB or a compact specimen with deep cracks i.e. pre cracks on the samples [42, 43].

J-integral method determines the J-integral as a crack extension (Δa). Then the J-integral was calculated from the area under the load vs displacement curve and the crack extension was calculated by single specimen (where a single specimen is tested with loading compliance technique i.e. with loading and unloading sequence applied to a sample) or multiple specimen technique (by considering many samples and performing the testes and braking the sample with different loads) shown in the Figure 2.2 (a,b) and the procedure and the explanation of the J-R curve method was explained by Hejazi et al. [44].

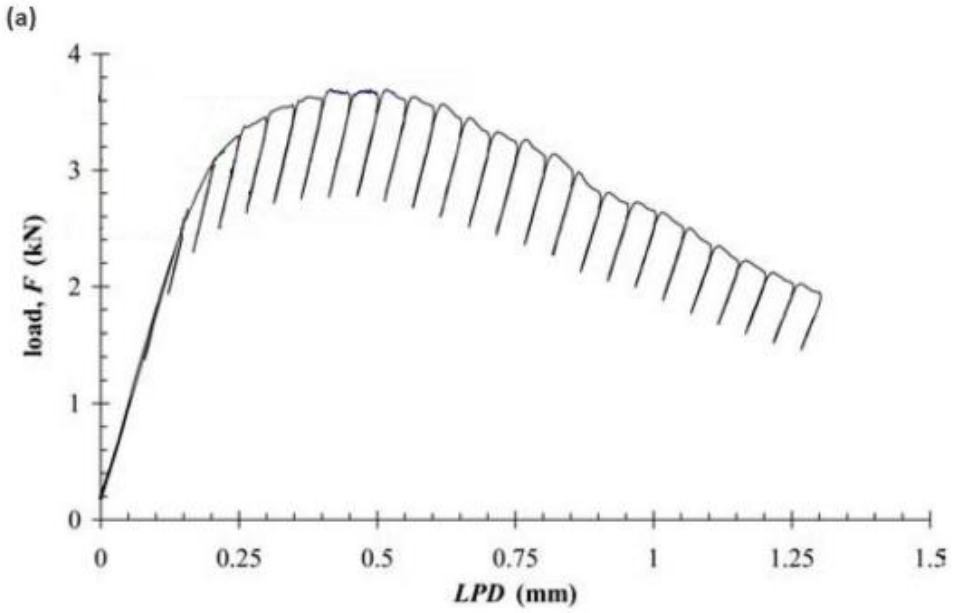

Figure 2.2: (b) Load F vs LPD (Load point displacement) for a single specimen technique [45]

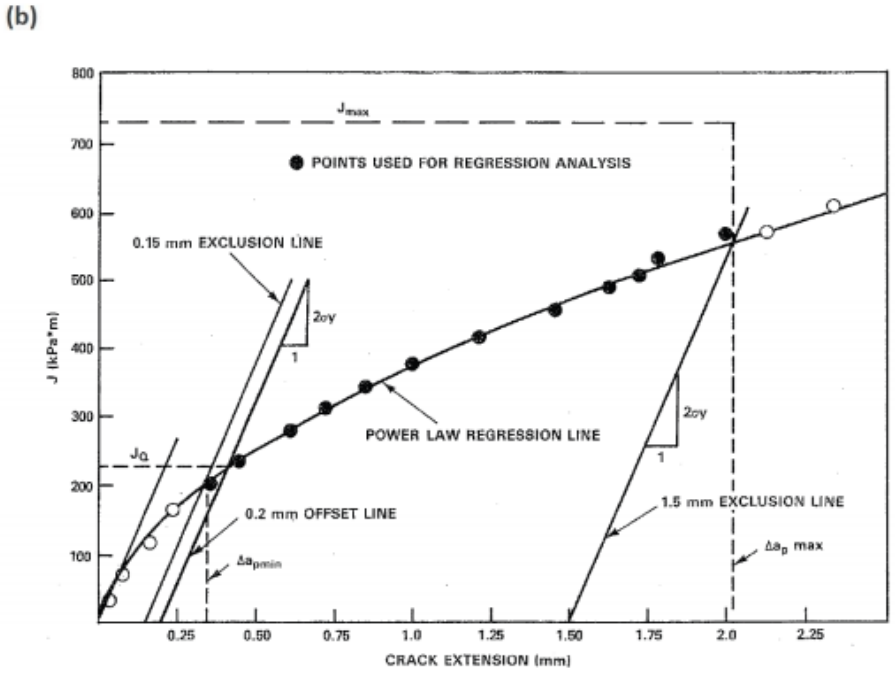

Figure 2.2: (b) J-R curve method used to determine JIC [46]

2.11 Re-appraisal of current problem

Now-a-days due to increasing demand of oil and gas industries, transportation of oil and gas for very long distances through line-pipe became common these days. From the application point of view HSLA steels are most suitable in which the mechanical properties can be easily altered by addition of micro alloying in required proportions to obtain the desired properties to the material based on the application so it is crucial to study the fracture toughness of the material because it plays a vital role. After a detailed survey on literature it was found that no report exists, which deals with the fracture toughness of welded API X65 grade steels. Hence, the current investigation is intended to study the fracture toughness of welded API X65 steels to fulfil this gap.

Chapter 3

Experimental procedures

3.1 Introduction

The aim of the present investigation is to study the facture toughness of welded high strength line-pipe steel in which the material chosen for investigation was API X65. To achieve this particular objective various tests were conducted which are discussed in this chapter. A brief overview of the tests conducted were determination of chemical composition of the selected steels, measurement of grain size and volume fraction of phases, determination of mechanical properties of the selected steel, microstructural characterization using optical and in transmission electron microscope in order to find out the second phases and precipitates respectively at various zones of the sample i.e. parent material, heat affected zone and weld zone. Harness profile of the sample was done in all the regions and in different welds as well which will be explained with the help of a stereo microscope image for better understanding, experiments related to fracture toughness, study of fractured surfaces in scanning electron microscope.

3.2 Material selection and chemical composition

Material used in this investigation was 10 mm thick hot rolled plates pertaining to API X65 grade where API stands for American petroleum institute. Plates of API X65 were received after rolling at Tata Steel limited. The chemical composition of the received plates was determined using optical emission spectrometer (ARL 3460).

3.3 Welding of the material

Pieces of dimensions 100 x 25 x10 mm were taken for welding. The welding was done with single bevel groove weld where different types of welds has been planned to be incorporated in this investigation. SMAW or conventional weld or stick weld fir root run followed by fill up of the joint by SAW. The cross sectional view of the sample is shown below in order to get a clear understanding of how the weld has been done Figure 3.1 which has been captured with LEICA M165C stereo microscope (Figure 3.2). The weld parameters along with consumables are discussed in the results and discussion. As the welds were not visible directly, some part of the sample was cut at the weld zone into 25x10 mm sample. The samples were prepared which will be explained briefly later in the microstructural examination.

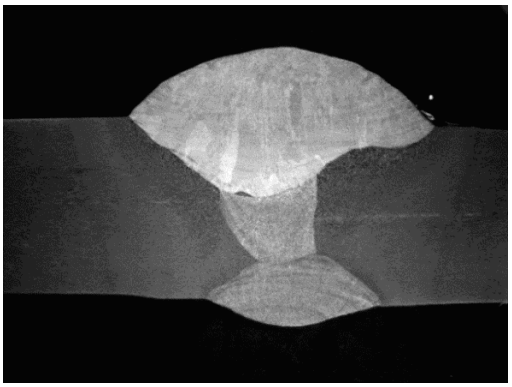

Figure 3.1: Cross sectional image of the material after weld

Figure 3.2: LEICA M165C Stereo microscope

3.4 Microscopic examinations and image analysis

As mentioned earlier in section 3.3 (Welding of the material) small portion of the welded sample was cut along the cross section. The sample of size 25x10 mm was cut with the help of Mecatome T-210 slow speed cutter. The latter is shown in the Figure 3.3.

Figure 3.3: Mecatome T-210 slow speed cutter

The mounting of the sample for microscopic observation was done with the help of Mecapress II specimen mount press (shown in the Figure 3.4) which is a hot mounting machine and takes around 20 min to mount the sample. The advantage of mounting the sample is ease of holding during polishing and handling. The mounting was done using conducting mounting material to facilitate SEM observation.

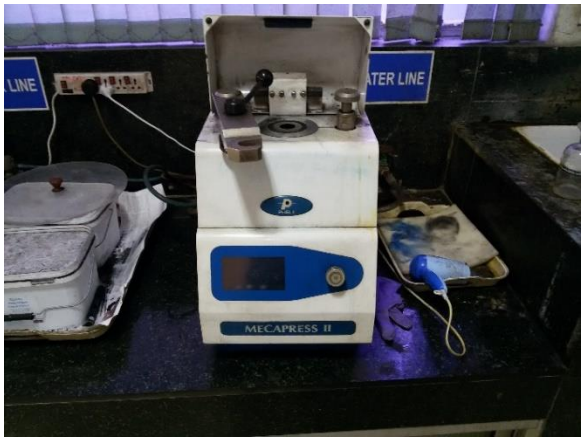

Figure 3.4: Mecapress II specimen mount press

Generally, two types of resins are used e.g. black coloured conductive resins and red coloured non-conducting resins. Although red resins (shown in Figure 3.5) are more economical to use, mounting with black resins is required if SEM examination is planned. Only samples mounted in black resins are conducting and are suitable for SEM.

Figure 3.5: Red and black resin powder used in the mounting of the sample

The mounted samples were polished using standard metallographic technique. First the samples were polished using different grades of emery papers (manufactured by Presi, made in France) with varying grit sizes namely 120, 180, 360, 600, 1000, and 1200. In order to remove the tapered ness and burr on the sample, grit sizes of 120,180 and 360 are used for very less time because material removal rate is very high in these papers of high grit size. Rest of the emery papers were used successively to remove the scratches on the sample surface. Polishing with emery papers were carried out using Mechatech Z64 semiautomatic polishing machine shown in Figure 3.6.

Figure 3.6: Mechatech Z64 semiautomatic polishing machine

In the above machines, there are disks to attach the emery papers and these emery papers are provided with glue in the back side to easily fix these on the discs. The polishing on emery papers was followed by polishing with 6µm, 3µm and 0.25 µm diamond slurry (supplied by FLACON MECAPREX LD 33E) using cloth as polishing surface in the same machine as mentioned above. The smooth, reflective and scratch-free sample thus obtained was cleaned with ethyl alcohol and dried with hot air blower. The polished sample was etched with 2% Nital (a solution of 2ml nitric acid HNO_3 in 98 ml ethanol) and then the sample was cleaned with ethyl alcohol and dried with hot air blower again. The sample was further etched with 4% picric acid (4gms picric acid ($(NO_2)_3C_6H_2OH$), 100ml ethanol).

The microstructures of the investigated material were examined with optical microscope shown in Figure 3.7 manufactured by LEICA (model: DM 6000M) with image analyzer software installed in the attached computer. With the help of image analyzer series of images were captured at different locations as mentioned earlier i.e. parent material, heat affected zone and weld zone respectively. The average grain size of the material was ASTM 10 and approximate phase fraction are shown in Figure 4.1.

Figure 3.7: LEICA DM 6000M with image analyser German made

3.5 TEM Analysis

In order to get better understanding of the second phases and precipitates present in the material TEM analysis has been done for the material. Thin samples of about 0.08 mm or 80 µm have been prepared by mechanical thinning process wherein care was taken not to introduce any bend in the samples. Thinned samples were etched with Nital in order to reveal the various zones on the sample. Punching of the sample has been done because the sample diameter is only 3mm that can be accommodated in sample holder of TEM equipment. The samples were punched in such a way that in all the different zones at least two samples can be obtained. After punching, electro polishing of the sample were done before loading the sample into the TEM. The process of electro-polishing has been explained briefly with the help of the Figure 3.8. For example, Figure 3.8 (a) shows the image of the sample after punching; Figure 3.8(b) shows the equipment used for electro-polishing (Tenopol-5 product of STRUERS) and Figure 3.8(c) shows the image of the samples after electro-polishing. Different parameters used while electro polishing are as follows: current: 30-40 milli ampere, voltage: 16V for first cycle for 30 sec followed by 19V for second cycle for 30 sec. Samples were cleaned with methanol before placing into the solution for electro-polishing i.e. Acitic acid 90% + Percolic acid 10%.

Figure 3.8: Explain the sequential procedure of electro polishing

The electro polished samples were loaded in the sample holder of TEM shown in Figure 3.9 model JEOL-2200FS Field emission electron microscope.

Figure 3.9: JEOL-2200FS Field emission electron microscope (TEM)

3.6 Hardness measurement

The sample was placed in the sample holder (Figure 3.10) securely prior to measurement of microhardness. Microhardness tester used in the present work (LECO model LM247AT Michigan, USA) is shown in Figure 3.11. The microhardness profile across the different zones of the weld region was evaluated.

Figure 3.10: Sample holder used for measurement of microhardness

Figure 3.11: The micro-hardness tester used in the present work

The hardness measurement of was made using load of 300 gmf for a dwell time of 10 Sec. The image of the sample after hardness measurement as captured with the help of a stereo microscope is shown in Figure 3.12. The image is incorporated for better understanding of the exact location of the sample where the hardness profile was estimated.

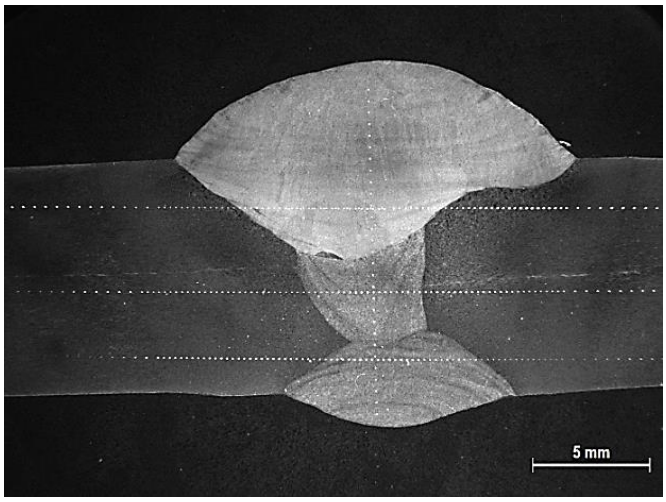

Figure 3.12: Image of sample after hardness indentations

3.7 Tensile test

Tensile tests specimen were fabricated according to ASTM- E08 [47] and were loaded to fracture on universal testing machine, model Instron 5582 shown in the Figure 3.13. The capacity of machine is 100 kN. Specimen ends were gripped and fixed in machine and its gauge length was continuously measured by advanced video extensometer (AVE) attached with the machine, until fracture.

Figure 3.13: Tensile testing machine used in the present work

3.8 Fracture Toughness Testing

Fracture toughness is the property of that describes the ability of a material containing a crack for resisting fracture. In case of brittle materials, linear elastic fracture mechanics (LEFM) is applicable and the toughness is usually defined as a value, which is characterized by the stress intensity factor K. Alternatively, for ductile materials, Elastic Plastic Fracture Mechanics (EPFM) has been developed. The toughness is defined either as a point value or as a resistance curve and is usually characterized by the J-integral. A J-integral based resistance curve i.e. J-R curve shows the resistance of a ductile material against crack initiation, its stable growth and tearing instability. This is the defined as J-controlled crack growth regime. To obtain a J-R curve from a single specimen test, an elastic unloading compliance technique is employed, wherein small elastic un-loadings

are applied periodically during the experiment and the change in compliance of these unloadings is used to estimate the crack length. This technique utilizes the phenomenon that as the crack length increases, the specimen compliance also increase i.e. its stiffness is reduced. Initially the sample was pre-cracked and loaded for fracture toughness test following ASTM E1820-13 standard [48] using a servo hydraulic test system (Instron model: 8850 shown in Figure 3.15. A representative sample after fracture toughness testing is shown in Figure 3.14.

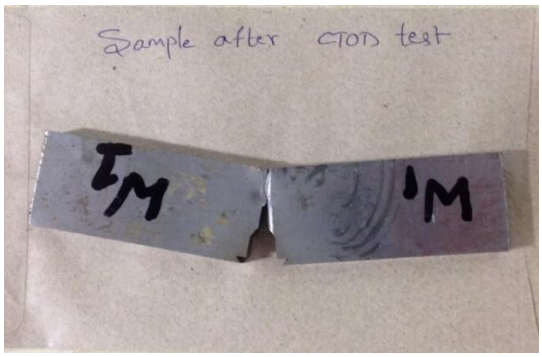

Figure 3.14: Broken sample after fracture toughness testing.

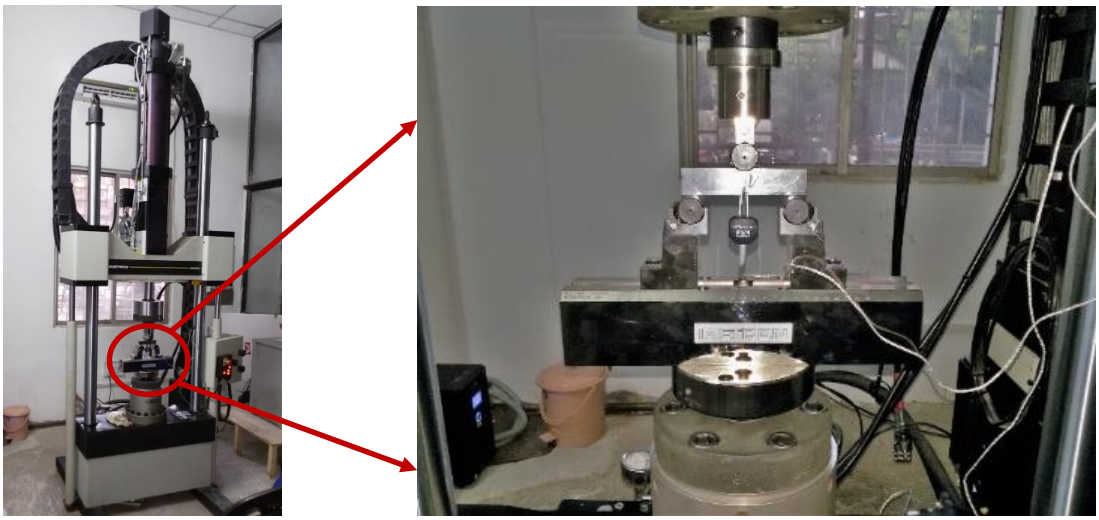

Figure 3.15: The servo hydraulic test system used for estimation of fracture toughness

3.9 Fractography

Fractography studies are important to analyze the mechanism of crack growth [49]. This becomes especially important for welded specimen in order to identify the location of crack initiation and the subsequent crack growth path. In the present work, failed specimens after fracture toughness testing were first examined with stereoscope to examine the macroscopic features of fractured surfaces. Thereafter, micro-fractography was carried out using a FE-SEM shown in Figure 3.16. The FE-SEM is manufactured by ZESIS (model supra 25). Before placing the fractured-sample in the FE-SEM, it was cleaned with ultrasonic cleaner. During fractography, microscopic features associated with crack-origin as well as crack growth path were documented by capturing relevant fractographs.

Figure 3.16: Image of FE-SEM (ZESIS SUPRA 25 German made)

Chapter 4

Results and Discussion

In this chapter, the obtained results from various characterization techniques are discussed along with their pertinent analyses.

4.1 Chemical composition

Plates of API X65 material were received from the hot roll mill of Tata Steel Ltd. with thickness of 10 mm each. The chemical composition was analyzed with optical emission spectrometer and the results are shown in Table 4.1. The chemical composition of the API X65 was compared with the API 5L standard [2]. The chemical composition of the material was in good agreement with the results reported by Hashemi et al. [50].

Table 4.1: Chemical composition of API X65 in weight %

Element	Weight %	API 5L
C	0.0541	0.430
Mn	1.4980	1.450
S	0.0011	0.015
P	0.0121	0.025
Si	0.2302	0.350
Al	0.0288	0.040
V	0.0355	0.080
Nb	0.0572	0.050
Mo	0.0860	0.250
N	54*	

*indicates that it is in terms of ppm (parts per million)

The nature of the precipitating elements and the micro alloying elements present plays a major role in the strength and toughness of HSLA steels. For example Nb, V, Ti used for grain refinement of the HSLA steels: these elements form precipitates and enhances grain refinement property in the steels [51]. Mo also serves the same purpose but by amalgamation of some amounts of Nb addition it increases the steel strength [52]. Mn increases the solid solubility of the steels but if Sulphur is present in steel, it forms MnS and the effects of MnS and contributes to reduction in ductility of the steels [53]. Therefore, the nature of precipitates and microalloyed elements plays a key role in the mechanical properties of the steel [54].

4.2 Tensile properties

The tensile tests were carried out on samples fabricated following the ASTM-E08 [47]. The procedure of tensile testing was explained in chapter 3. Specimen ends were gripped in the machine up to the gauge length marked with two white dots the calibrated distance between the two white dots was continuously measured by advanced video extensometer (AVE) attached to the machine till fracture and the readings are obtained in the system attached to the machine. The obtained tensile properties were summarized in the Table 4.2

Table 4.2: Tensile properties of API X65

Sample Number	Yield Strength (MPa)	Ultimate Tensile Strength (MPa)	Uniform elongation (%)	Elongation at fracture (%)
1	465.53	571.41	11.57	30.23
2	464.00	570.76	12.01	30.65
3	477.84	570.85	11.65	30.01

4.3 Microstructure and grain size determination

After welding of the material the sample was prepared as explained earlier and the microstructural analysis was done with a optical microscope (Model: LEICA DM 6000M with image analyzer made in Germany).

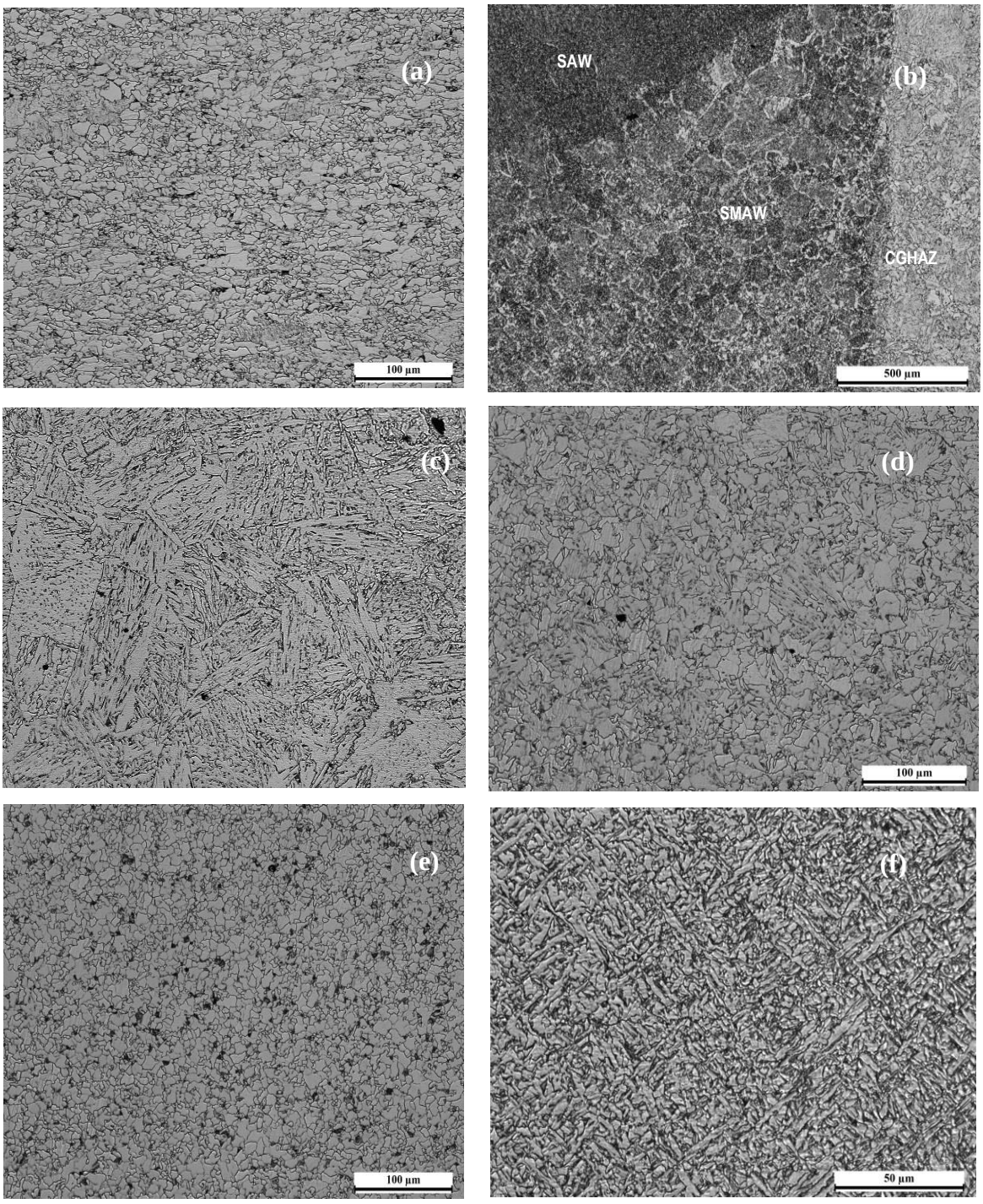

Figure 4.1: Detailed microstructure of API X65 weld

The detailed microstructure of weld one is shown in Figure. 4.1. Figure. 4.1(a) shows the parent material microstructure comprising of ferrite and other second phases. As mentioned earlier, the ratio of ferrite to second phases is approximately 9:1. Figure. 4.1(b) shows the SAW, SMAW and CGHAZ region (coarse grain heat effected zone) of the weld. Figure. 4.1(c) and (d) show the CGHAZ and slightly coarsened HAZ region, wherein prior austenite grain boundaries can be observed. Figure 4.1(e) further away fine grain HAZ is observed. Figure. 4.1(f) shows acicular ferrite microstructure. In order to better understand the second phases and precipitates, transmission electron microscopy was carried out and results are discussed in Figure.4.3.

The average grain size of the base material was found to be 10 µm which also satisfies the ASTM standard and also reported by Fragiel et al. [55]. By this there was approximately 91% of ferrite and 9% of second phases shown in Figure.4.2

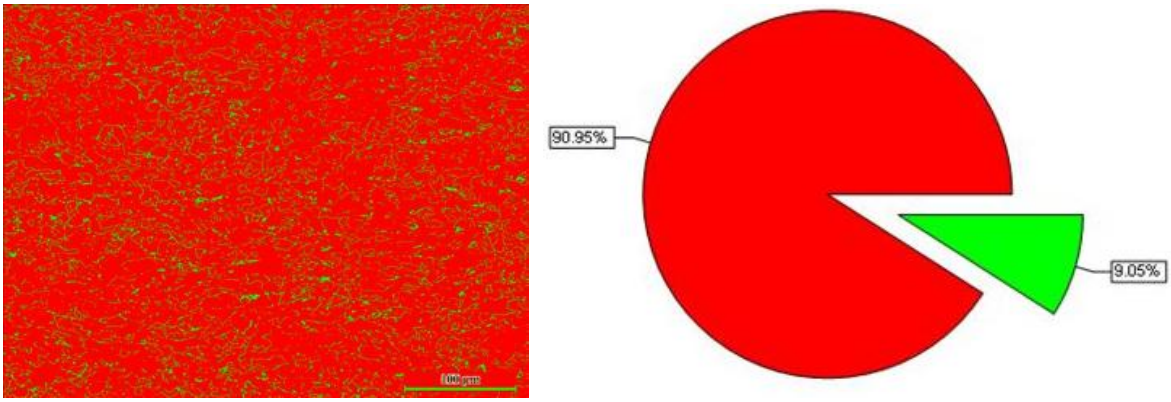

Figure 4.2: Representative Figure and phase fraction for APIX65

As there are some precipitates present in the material it is very difficult to directly know the second phases present in the material so futher investigation was performed by using transmission electron microscopy by this the second phases and precipitates were found out.

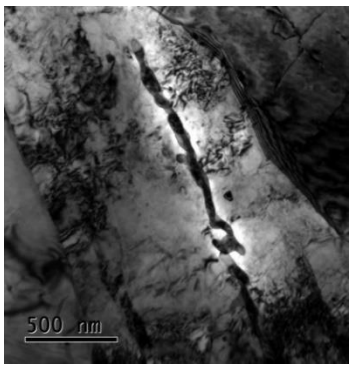

(a)Bainitic sheave with coarse carbide

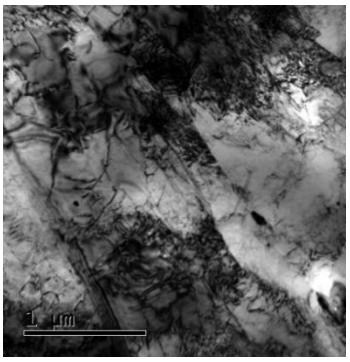

(b) Polygonal structure

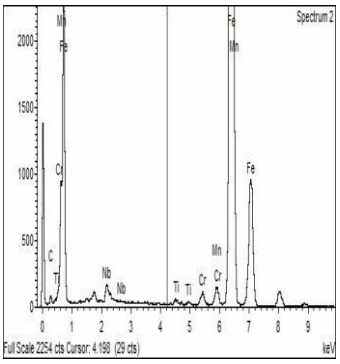

(c) EDX of precipitate – NbC

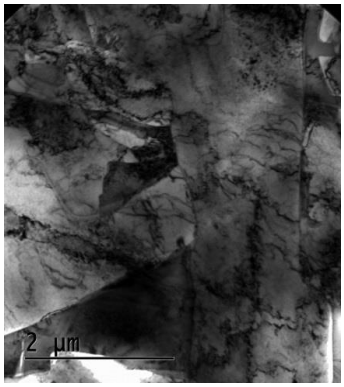

(d) Acicular ferrite

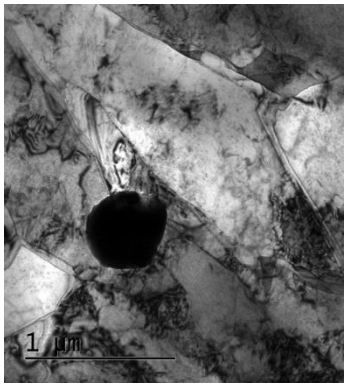

(e) Inclusion and AF

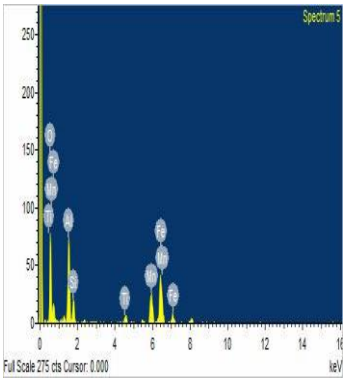

(f) EDX of precipitate – Al_2O_3

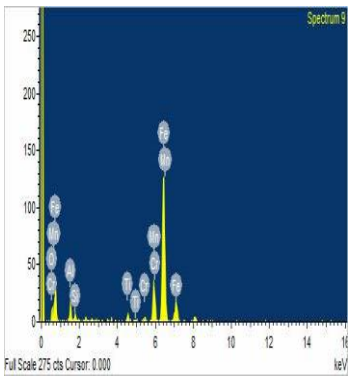

(g) EDX of precipitate-complexTiO_2

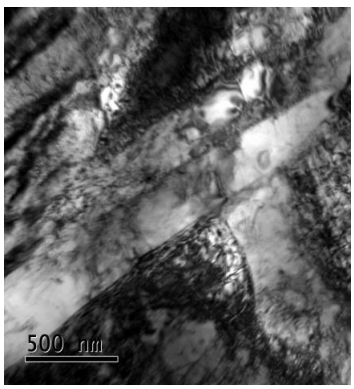

(h) Bainitic sheaves

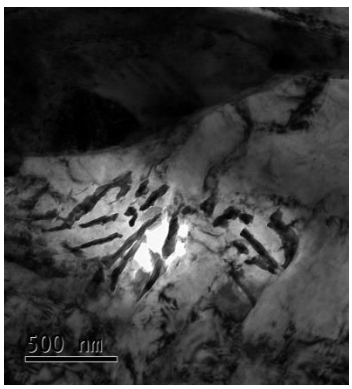

(i) Coarse Fe_3C

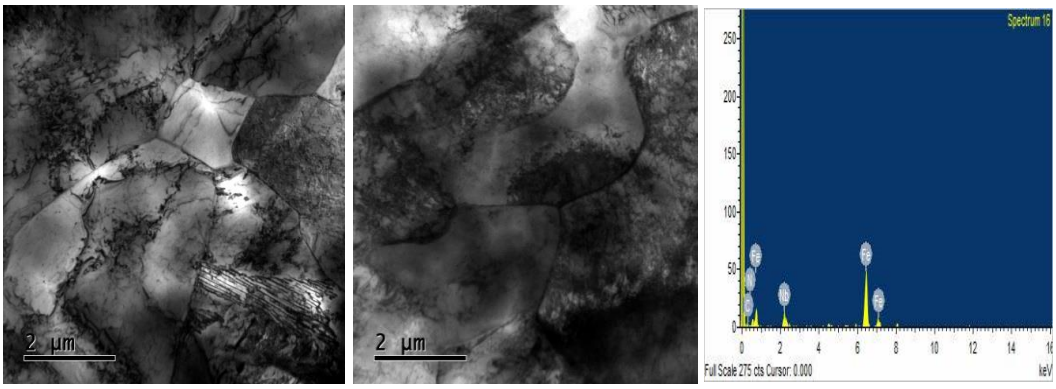

(j) Polygonal structure (k) GB decorated with Fe_3C (l) EDX of precipitate – NbCN

Figure 4.3: (a)-(c) base material; (d) to (g) weld region; (h) & (I) coarse HAZ and (j)-(l) fine HAZ

In order to analyze the microstructure in and adjacent to weld zone in APIX65 steel, TEM analysis was carried out to identify the different microstructural phases (Figure. 4.3). Bainitic sheaves were observed in parent material, weld zone, grain coarsened and grain refined region. Acicular ferrite was seen in weld region and it nucleated on inclusion namely Al_2O_3 and complex TiO_2 types. Coarsened carbides particles (Fe_3C) were observed in parent material and also in heat affected zone. Niobium carbide and niobium carbonitrides precipitates were observed in parent material and also in grain refined region but not in grain coarsened region, where it is possible that these precipitates were dissolved.

Ferrite/ proeutectoid ferrite is formed during the slow cooling from austenite at the highest transformation temperature. Increasing the cooling rate lead to different kinds of ferrite phases. At slow cooling, ferrite grains form precipitated at austenite grain boundaries which leads to polygonal ferrite formation. At higher cooling rates ferrite loses its polygonal structure and forms elongated crystals termed as Widmanstatten ferrite (WF). Further increasing the cooling rate will lead to formation of massive ferrite or quasi polygonal ferrite.

Bainite has named after the report submitted by Davenport and Bain in 1930 [56] where there are six classifications in bainite which was reported by Reynolds in 1991 [57] of this two were mostly acknowledged they are lower bainite and upper bainite i.e. if the cementite was formed inside the bainitic ferrite it is termed as lower bainite at lower temperature and if cementite was present at the grain boundaries of the bainitic ferrite it is termed as upper bainite at higher temperatures. Acicular ferrite was first reported by Smith in early 1970`s [58] noted for its high dislocation density and fine grain nature leads to good mechanical properties like good strength, corrosion resistance and good toughness at low temperature. Acicular ferrite will have ferrite plates randomly placed with prior austenite grains [59]. This was formed upon rapid cooling of low carbon steels where there are ferrite plates with long elongated morphology which is quite different from that of polygonal ferrite. The formation of acicular ferrite depends on the cooling rate as mentioned earlier it also depends on the amount of deformation on the rolling passes tells the volume fraction of acicular ferrite produced, the larger the deformation the higher the transformation temperature then the higher the amount of acicular ferrite in microstructure.

4.4 Hardness profiles of API X65 welded sample

Hardness test was carried out for the samples prepared as mentioned in chapter 3. For better understanding, the stereoscope image of the sample indentation is illustrated in Figure.4.4. Hardness profiles was done with HV-300 gf and dwell time of 10Sec for APIX65 base metal and weld joint shown in Figure 4.5 (a) and (b).

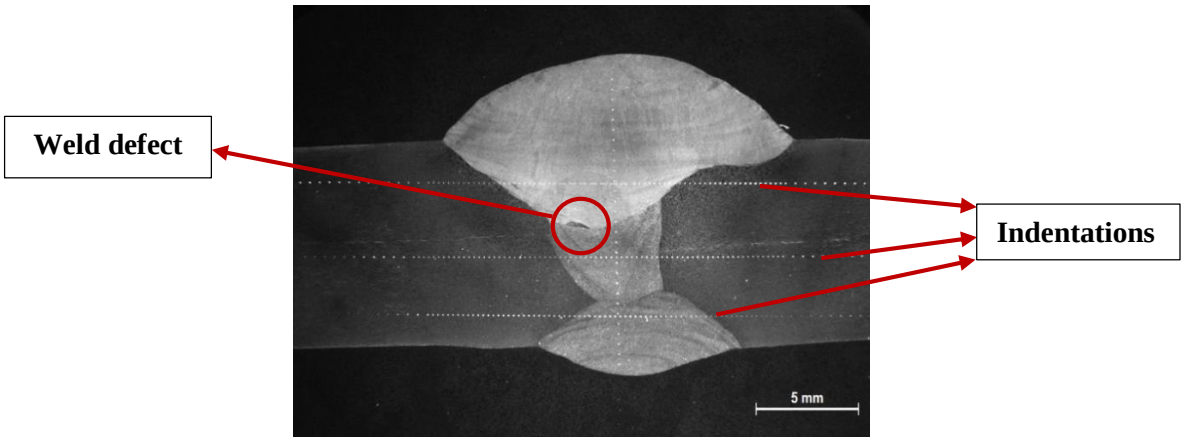

Figure 4.4: Image of the sample after indentations

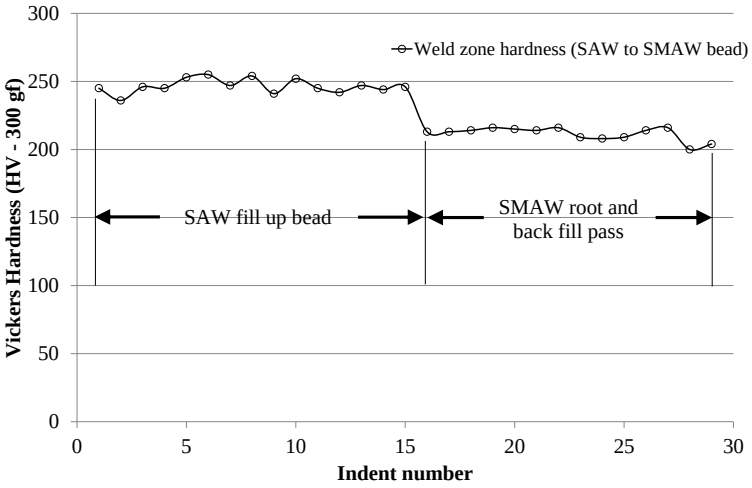

Figure 4.5 (a): Hardness profile vertically top to bottom in weld zone

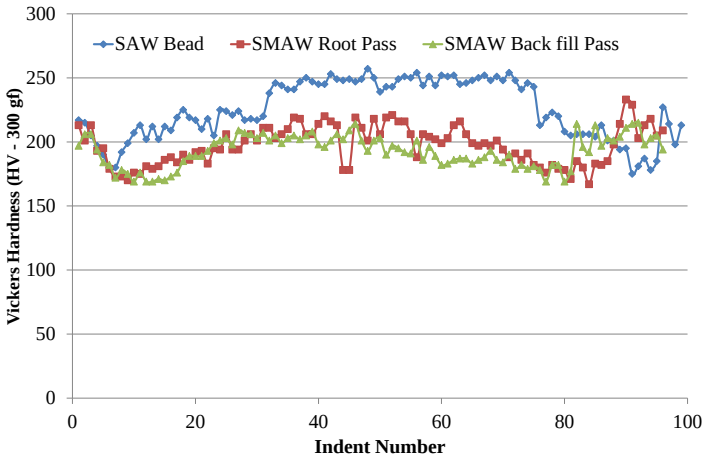

Figure 4.5 (b): Hardness profiles horizontally across weld zone

In Figure 4.5(a), hardness measurements from top to bottom in the weld zone is shown, it can be seen that despite similar all weld metal strength, the hardness drops by 35 VHN in SMAW deposit and this can be attributed to tempering effect of the SAW fill up pass. From microstructural point of view the higher hardness in the weld region is due to the presence of acicular ferrite in the weld region. Weld hardness across the weld zone along SAW fill up, SMAW root pass and SMAW back pass are shown in Figure 4.5(b). A dip in hardness is observed approximately 10 mm away from the weld zone which is HAZ (heat effected zone). The hardness value of HAZ is slightly lower than that of BM (base metal) and a bit lesser than that of the weld region, this is due to the presence of bainite, polygonal ferrite and acicular ferrite in the HAZ region. During welding, these HAZ region will not experience any melting, but there will be microstructural changes due to phase transformation shown in the Figure 4.1 (c, d, e). The grain size was varied with the distance from the fusion line. The coarseness in the microstructure was due to the heat input of the SAW and SMAW welding processes. From this low hardness value of the HAZ compared to BM explains slightly softening of HAZ in API X65 weldment reported by Hashemi et al. [60]. Similarly HAZ softening for this steel was reported by Lee et al. [61]. It should be noted that tensile properties of the HAZ region was not reported by the API standard [2]. It is very difficult to determine the strength levels in HAZ which requires special testing equipment. However Lee et al. reported that some micro-tensile experiments can determine tensile properties in HAZ [62].

4.5 J-R curve tests on welded API X65 plates

Fracture toughness of API X65 plates were carried out as per ASTM E1820 [48]. Three point bend specimen geometry was selected and dimensions are shown in Figure. 4.6. Notch was placed in weld zone, fusion line and heat affected zone beside tests conducted for parent material. These regions were identified by etching the EDM cut sample and marking the selected region for notch cutting.

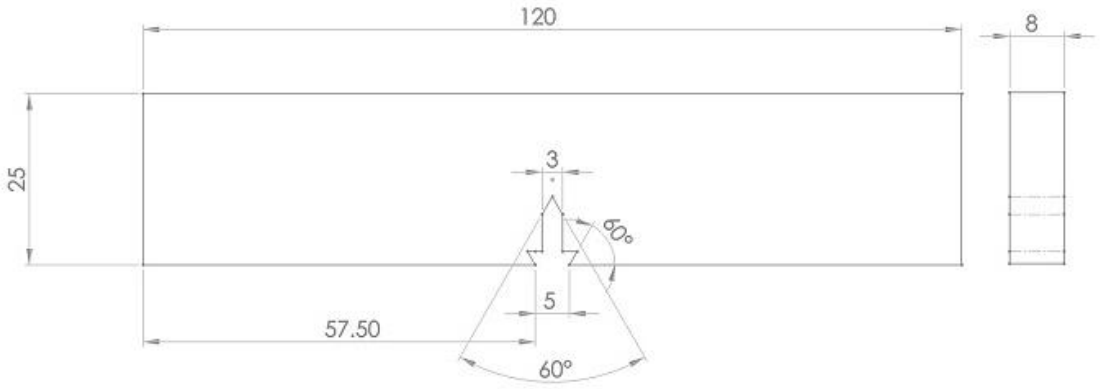

Figure 4.6: Three point bend specimen for J-R curve testing

Tests were conducted at a cross head velocity of 0.008 mm/min. Two samples were tested for each selected zone. J-Integral method determines the J-value as a function of crack extension (Δa).

The J-value is calculated from the area under the load-displacement curve and crack extension. This be measured by either multiple specimen technique where different samples are tested to different loads and break all the samples to measure the crack length manually. The current investigation is conducted using a single specimen for the J-integral tests.

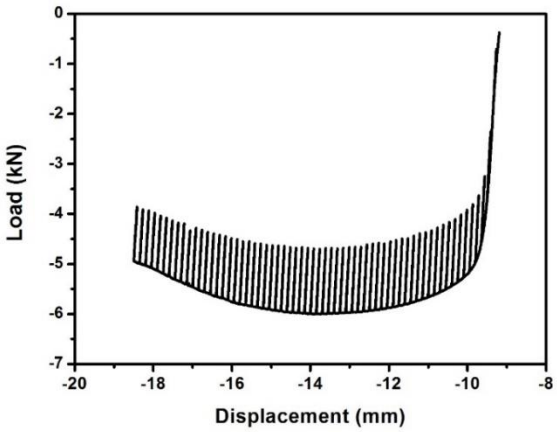

Figure 4.7 (a): Load vs displacement obtained from the data collected from the equipment

The load applied was in the negative direction as shown in Figure 3.14. The load was applied from top to bottom by taking the set value as zero before loading the sample so all the values obtained from the machine are in the negative direction. The results are shown in Figure 4.7 (a) and by changing the symbol of the obtained results the graph was turned to the positive planes of the X,Y axis as shown in Figure 4.7 (b).

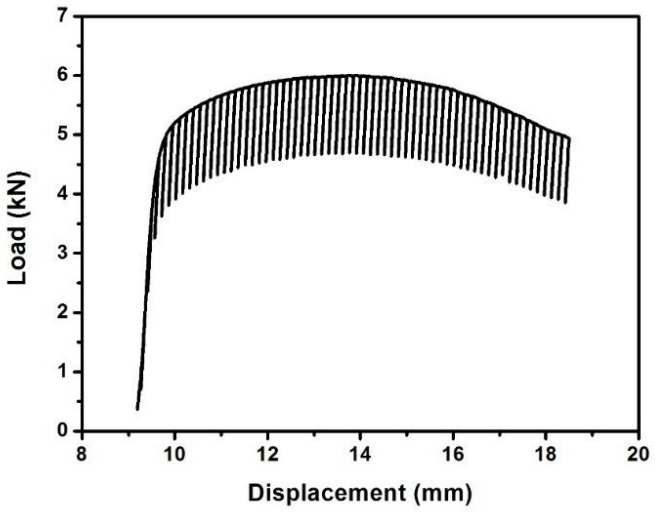

Figure 4.7 (b): Load vs displacement plot modified to match with standard

Representative J-R curves for weld and heat affected zone, are shown in Figure. 4.8. The area under the curve represents the energy observed by the specimen before fracture, which indicates that toughness of heat affected zone is superior to weld zone. Based on analysis of the obtained curves the J_Q values for different regions are listed in Table 4.3.

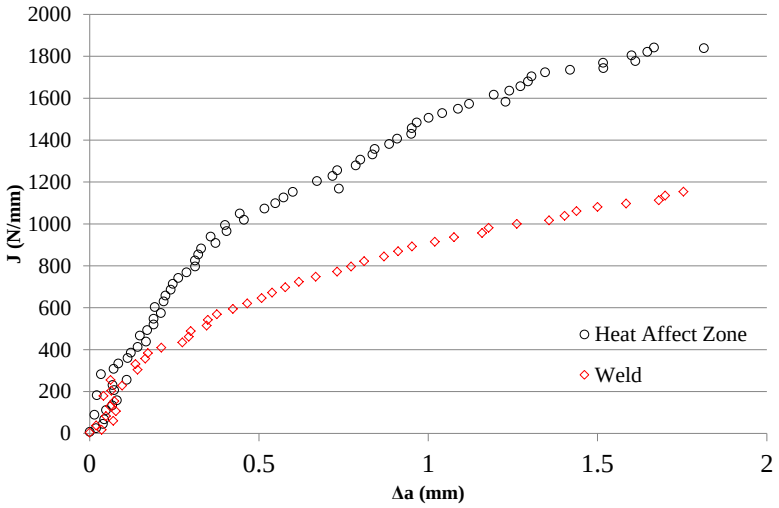

Figure 4.8: Representative J-R curves for weld and heat affected zone

The fracture toughness testing was done for each sample and the obtained results are tabulated below in Table 4.3 which shows the J_Q values in different zones.

Table 4.3: J_Q value obtained for different regions of welded API X65

Region	J_Q value (N/mm)
Base Material	1960
	1925
Weld zone	940
	890
Fusion line	1425
	895
Heat affected zone	1940
	1910

From Table 4.3 we can find out the fracture toughness of the material ranging from 890 to 1960 N/mm respectively. There is no significant change in the toughness values in between base material and heat affected zone. As there is no much variation in microstructure in base material and in heat affected zone the toughness values are also almost similar. At room temperature all the values that are required to obtain J_Q values

have exceeded the API standard 1104 and DNV-OS-F101 standard [62, 63]. The J_Q values of weld zone are about 53% lower than that of base material. The value for fusion line samples are significantly different i.e. 1425 and 895 N/mm indicating an average reduction of 40% in J_Q value as compared to base material. The scatter in fusion line value can be attributed to error in precise placement of notch or deviation in crack growth path during testing. The difference in J_Q values in the weld zone may be due to the presence of defect in the weld nugget as from the stereo microscope image shown in Figure 4.4. Despite the excellent toughness at various zones, there was a huge difference between the base metal and weld zone because of the weld defect present in the filled up weld done with submerged arc welding process and due to this, the criterion of uniform crack front and uniform crack growth may not be satisfied. The results obtained are used to determine the crack length and if there is non-uniformity in the crack growth it leads to less accurate crack estimations. In this study all the samples were tested with constant thickness so comparison of the samples was valid, as the geometry of all the samples is same.

4.6 Fractography of fracture toughness tested broken samples

The fractographic tests of different broken samples after fracture toughness tests are done in FE-SEM. Typical fractographs are illustrated in Figure 4.9. As one can see from Figure 3.16 the fracture toughness tested samples did not completely break during the test, these were broke by putting the sample in liquid nitrogen for about 1min followed by hammering. It is known that introduction of liquid nitrogen makes a steel brittle thereby makes it easier to break. Figure 4.9 (a) shows the two broken halves of the single edge notch (bend) specimen. One can clearly note the notch region (represented by ‘N’ in the figure) fatigue pre-crack region (represented by ‘FP’) crack growth region (represented by ‘CG’) and final failure (represented by ‘FF’). Figure. 4.9(b) shows a magnified view of sample highlighting the fatigue pre-crack and crack growth region; it also shows the measurement of fatigue pre-crack front which gives the initial value of crack for the final J-R curve test. Figure. 4.9(c) mainly shows the crack growth region. Figure. 4.9(d) shows fatigue striations present in fatigue pre-crack region. In this the presence of secondary

micro cracks and slips planes considered as typical fatigue crack surface of API X65 material with fatigue striations present in this region. It is evident from the images that the fracture occurred shown in Figure 4.9(e) is a higher magnification image of very fine dimples present in coarse grained heat effected zone indicating ductile fracture with having very high fracture toughness which is in agreement with Jang et al. [64].

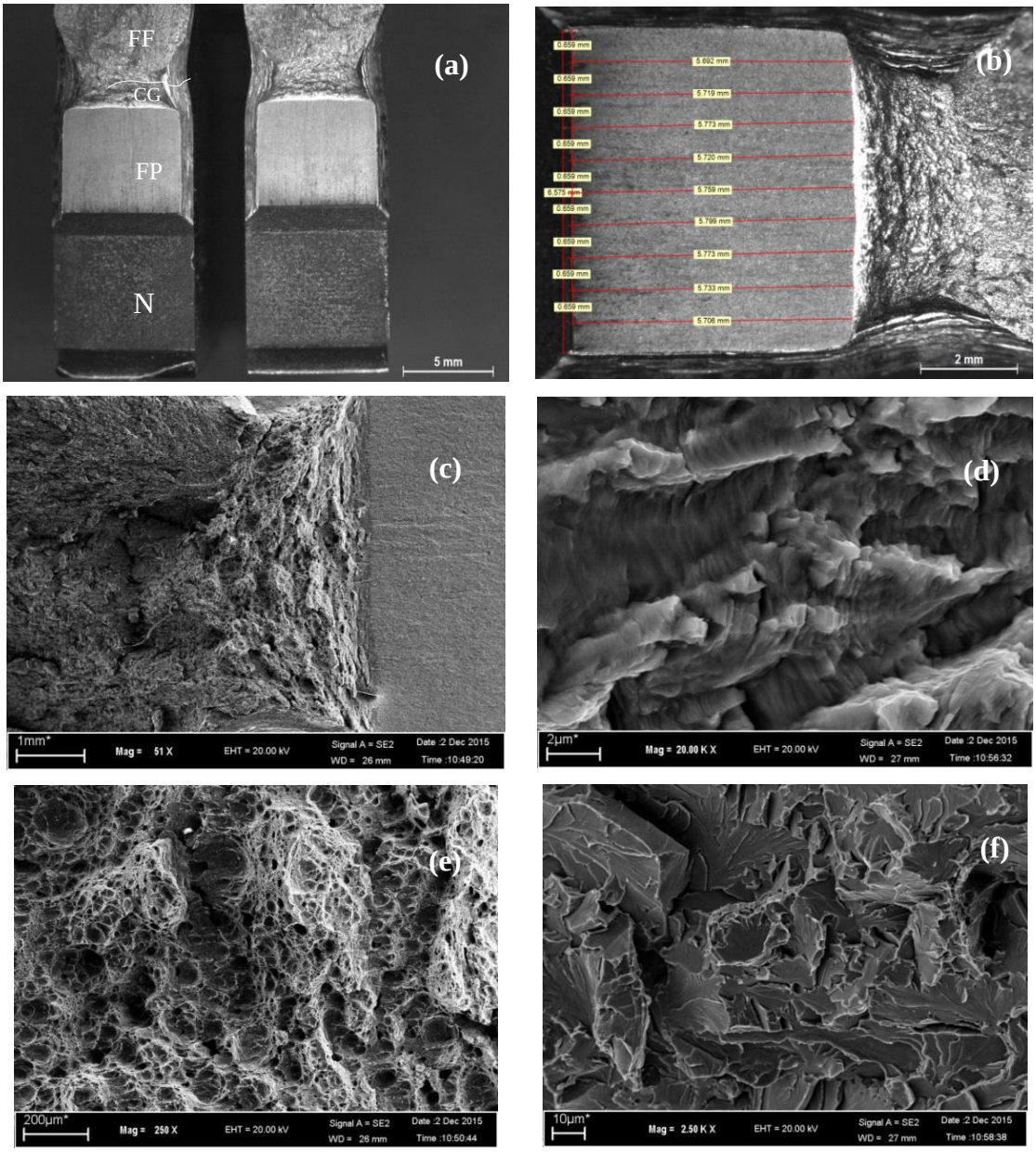

Figure 4.9: Stereoscopic and SEM micrographs of different regions of tested three point bend J-R curve sample

It is reported that the fracture occurred in API 5L series consists a brittle to ductile transition i.e. the fractures initiates with brittle fracture (trans granular cleavage) and later is arrested by ductile region [65] . In API series the failure mode for fracture toughness was ductile fracture due to the ductile behavior of API X65 material. Obviously by the fractographic study shown in figure 4.9(e) with dimples it is evident supporting for this conclusion. Figure 4.9(f) shows the final fracture caused by striking the sample with a hammer after dipping it in liquid nitrogen. The brittle cleavage morphology can be observed from this fractograph; but this is of no effect in the fracture toughness of the material as it has been performed for convenience for fractographic study.

Overall, different characterizations were done for API X65 steel. This include chemical composition, tensile properties, microstructural analysis, TEM analysis, fracture toughness tests, fractography. The obtained results indicated that the steel is a good candidate for use in line-pipe steel and its weld.

Chapter 5

Conclusion and future scope

5.1 Conclusions

The aim of this investigation was to evaluate the fracture toughness of welded API X65 steel plates keeping in view the limited number of reported works on the subject. The selected steel was characterized in terms microstructure, hardness and tensile properties. The welding of steel plates was performed with sub merged arc welding (SAW) with root pass of shielded metal arc welding (SMAW). The microhardness profile in. base material (BM), heat affected zone (HAZ), weld zone (WZ) and weld nugget were evaluated. The microstructural features of the above zones were revealed using optical and transmission electron microscopy. The fracture toughness of the above zones of welded plate was evaluated in terms of J-R curve following the concept of EPFM. Major conclusions are:

- The evaluation of fracture toughness of welded API X65 indicates that, J_Q value of heat affected zone was slightly lower than the base material, but for the weld zone it dropped significantly by 53% due to the non-uniform crack front and crack propagation. The phenomenon is attributed to presence of different defects in the weld region.
- J_Q value for fusion line samples showed significant scatter with an average reduction of 40% in J_Q value as compared to base material. The scatter in fusion line value can be attributed to error in precise placement of notch or deviation of crack path during testing.
- Presence of Nb and V imparts precipitation hardening effect to the API X65 steel, such that it has a satisfactory combination of strength and toughness parameters fulfilled by API service requirements.

Future scope

5.2 Scope for future research

- Study of Fatigue crack growth rate tests (FCGR) can be performed on this material with same welds.
- Study of fracture toughness with different combinations of conventional welding techniques can be performed.
- Fracture toughness variations with changing weld parameters like welding speed and wire feed rate etc. can be performed.
- Study of fracture toughness tests can be performed by welding as spiral submerged arc welding process with varying thickness by comparing the toughness values one can recommend the best thickness for practical applications in oil and gas industry.

Bibliography

1. Li. L and Xu. L. "*Designing with High-Strength Low-Alloy Steels. In: Handbook of Mechanical Alloy Design*". Marcel Dekker, Inc.; 2004. p. 249-320. PMC id: PMC3090257.
2. American Petroleum Institute. Specification for Line-pipe. ANSI/API Specification 5L. 44th ed. American Petroleum Institute; 2008.
3. A. G. Barkow, "*Columbium Steel in High-Pressure Line-pipe Service*", AISI Regional Technical Meeting No. 59, Buffalo, N.Y., 1960. See also U.S. Patent No. 3,010,822, Nov. 1961.
4. https://en.wikipedia.org/wiki/High-strength_low-alloy_steel retrieved 25-01-2016.
5. https://en.wikipedia.org/wiki/High-strength_low-alloy_steel retrieved 25-01-2016.
6. "*Degarmo`s, Materials processes and manufacturing*" p. 116.
7. "*Stainless steel properties for structural automotive applications*" . Euro Inox. Retrieved 25-01-2016.
8. "*High strength low alloy steels understanding the basics by ASM International*": 2001.
9. *"Classification of Carbon and Low-Alloy Steels*", retrieved 25-01-2016 Total Materia article.
10. H. Rampaul, "*Pipe welding procedures 2ed. 2003*", New York industrial press. 190
11. G. M. pressouyre, J. P. Fidelle, "*Hydrogen effects in metals in international conference of effect of hydrogen on behavior of materials*". 1980, Metallurgical society of AIME: Moran, Wyoming. P 27-36.
12. C. C. Anya, T. N. Baker, *"The effect of silicon on the grain size and the tensile properties of low carbon steels"*. Materials science and engineering: A, 1989, 118; p. 197-206.
13. S. Serajzadeh, A. K. Taheri, "*An investigation on the effect of carbon and silicon on flow behavior of steel. Materials and design*", 2002, 23(3); p, 271-276.
14. K. Ravi, V. Ramaswamy, T. K. G. Namboodhiri, "*Effect of molybdenum on the resistance to H_2S of high Sulphur Microalloyed steels*", Materials science and engineering: A, 1993.169(1-2); p.111-118.
15. J. Kong, C. Xie, "*Effect of molybdenum on continuous cooling bainite transformation of low carbon Microalloyed steel*". Materials and design, 2006. 27(10): p.1169-1173.

16. J. C. Cao, Q. Y. Liu, Q. I. Yong, X. J. Sun, "*Effect of Niobium on Isothermal Transformation of Austenite to Ferrite in HSLA Low-Carbon Steel*". Journal of Iron and Steel Research, International, 2007. 14(3): p. 52-56.
17. J. G. Williams, C. R. Killmore, P. D. Edwards, P. G. Kelly, "*Thermomechanical processing of Mo-Nb high strength steels for applications to X70 and X80 ERW line-pipe*", in 2nd international conference on Thermomechanical processing of steels and other materials (THERMEC 97), T. Chandra, T.Sakai, Editors.1997, "*Minerals, Metals & Materials Society*": Wollongong, Australia. P. 475-482.
18. K. Denpo, H. Ogawa, "*Effects of nickel and chromium on corrosion rate of line-pipe steel*". Corrosion science, 1993. 35(1-4): p. 285-288.
19. M. Gomez, L. Rancel, S. F. Medina, "*Effects of aluminium and nitrogen on static recrystallization in V-Microalloyed steels*". Materials science and engineering: A, 2009. 506(1-2): p. 165-173.
20. L. Savov, E. Volkavo, D. Janke, "*copper and tin in steel scrap recycling Materials geoenvironment*", 2003. 50(3): P. 627-640.
21. C. L. Briant, "*The effect of nickel, chromium and manganese on phosphorous segregation in low alloy steels*", Scripta Metallurgica, 1981. 15(9): p.1013-1018.
22. S. S. Kojima, M. A. Sampaio, I. S. Bott, "*The development of API 5L X80 steel for pipe production by TMCR process*", T&B petroleum, Year 5 - Number 15, 2003.
23. J. F. Evans, M. T. Clark, "*Plate cooling – Technologies and market requirements*" AISE Steel technology, June 2002.
24. P. A. Peters & J. M. Gray, "*Genesis and Development of Specifications and Performance Requirements for Modern Line-pipe - Strength, Toughness, Corrosion Resistance and Weldability*", Australian Pipeline Industry Association, Inc. 1992 International Convention; Hobart-Tasmania, Australia; October 24-29, 1992.
25. J. M. Gray, P. A. Peters, "*Technical Demands and Specifications for Line-pipe During the Past Decades*". CBMM/TSNIICHERMET Seminar - 25 Years of Cooperation. Moscow Russia. September 5-6, 2002.
26. J. M. Gray, F. Siciliano "*High Strength Micro alloyed Line-pipe: Half a Century of Evolution*". Micro alloyed Steel Institute 5100 Westheimer, Suite 540, Houston, TX 77056 USA 2008.
27. C. L. Coffin from Detroit firstly patented on "Process of welding metals electrically" US patent number-428459 A, published date May 20 1890.
28. Y. Shinohara, Y. Nagata, E. Tsuru, T. Hara, "*Evaluation for Fracture Toughness in Welded X80 Pipes: Experimental Analysis on Mechanical Properties of HAZ*". Twenty-first (2011) International Offshore and Polar Engineering Conference. Maui, Hawaii, USA: International Society of Offshore and Polar Engineers; 2011.

29. X. Xu, Y. Su, W. Zhou, Q. Cai, "*Relationship Between M--A Constituent and Cleavage Fracture Behaviour of Granular Bainitic Weld Metal*". Acta Metals in (EnglEd) A. 1989;2:143-6.
30. D. R. Johnson, W. T. Becker, "*Toughness of tempered upper and lower bainitic microstructures in a 4150 steel*". Journal of Materials Engineering and Performance. 1993;2: 255-363.
31. J. Shimamura, M. Okatsu, N. Ishikawa, K. Nishimura, Y. Murakami , S. Tsuyama, "*Material Design Concept in Heavy Wall X100 High Strength Line-pipe Steel*". Twenty first (2011) International Offshore and Polar Engineering Conference. Maui, Hawaii, USA: International Journal of Offshore and Polar Engineering; 2011.
32. J. L. Theodore, H. E. Kennedy, M. A. Rothermund, "*Electric welding*" patent number US 2043960, published on 1935-10-09, issued 1936-06-09.
33. J. G. Garland, P. R. Kirkwood, "*Towards Improved Submerged Arc Weld Metal, Metal Construction*", May 1975, p. 275-283 and June 1975, p. 320-330.
34. E. Levine, D. C. Hill, "*Structure-Property Relationships in Low C Weld Metal*", Metallurgical Transactions, September 1977, p. 1453-1463.
35. C. L. Choi, D. C. Hill, "*A Study of Microstructural Progression in As-Deposited Weld Metal*", Welding Journal, August 1978, p.232s-236s.
36. S. Liu, S. L. Olson, "*The Role of Inclusions in Controlling HSLA Steel Weld Microstructures*", Welding Journal, June 1986, p. 139s- 149s.
37. P. K, Ghosh. P. K. Singh and N.B. Potluri, "*Fracture Properties of Multipass Submerged Arc Steel Produced by Using Flux Cored Filler Wire Weld of HSLA*" ISIJ International, Vol. 38 (1998), No. 12, pp. 1379-1386.
38. H. S. Lu, Y. H. Yang, G. Chen, X. Chen, X. Wang., "*Fracture toughness of different locations of spiral submerged arc welding joints in API X80 pipeline steels*" 14th International conference on pressure vessel technology , Procedia engineering 130 (2015) 828-834.
39. B. Beidokhti, A. H. Koukabi, A. Dolati, "*Effect of titanium addition on the microstructural properties and inclusion formation in submerged arc welded HSLA steels*", Journal of Materials Processing Technology 209 (2009) 4027–403.
40. D. V. Kiran, B. Basu A. De., "*Influence of process variables on weld bead quality in two wire tandem submerged arc welding of HSLA steels*" Journal of materials processing technology 212(2012): 2041-2050.
41. ASTM E399-90, "*Standard test method for plane-strain fracture toughness of metallic materials*", Annual book of ASTM standards 3.01, American society for testing and materials, west Conshohocken, PA (1997).

42. J. R. Rice *"A path independent integral and the approximate analysis of strain concentration by notches and cracks*". Applied mechanics 1968; 35:379–386.
43. J. W. Hutchinson "*Fundamentals of the phenomenological theory of nonlinear fracture mechanics journal of applied mechanics*", 1983. 50(4b): P.1042-1051.
44. D. Hejazi "*Effect of manganese content and microstructure on the susceptibility of X70 pipeline steel to hydrogen embrittlement*". 2014. P 40-44.
45. R. Chaouadil "*An energy-based crack extension formulation for crack resistance characterization of ductile materials*". ASTM Journal of testing and evaluation, 2004.32(6): p. 469-475.
46. ASTM E813-89: "*Standard Method for J_{IC}, A Measure for Fracture toughness*". 1989.
47. ASTM E08-09, "*Standard Test Methods for Tension Testing of Metallic Materials*", ASTM International, 100 Barr Harbor Drive, P.O.Box C700, West Conshohocken, PA 19428–2959,United States, 2009.
48. ASTM E1820 "*Standard test method for measuring of fracture toughness*", ASTM International, 100 Barr Harbor Drive, P.O.Box C700, West Conshohocken, PA 19428–2959,United States, 2013.
49. D. Hull, "*Fractography: Observing, Measuring and Interpreting Fracture Surface Topography*", Cambridge University Press, 23-Sep-1999.
50. S. H. Hashemi, D. Mohammadyani, "*Characterisation of weldment hardness, impact energy and microstructure in API X65 steel*". International journal of pressure vessels and piping 2012.
51. H. T. chi. "*Newly Developed High Strength Steels in Japan*", HSLA Steels: Processing, Properties and Applications, The Metals & Materials Society, @ 1992 p 33-36.
52. A. M. Sage, "*An Overview of the use of Microalloys in HSLA Steels with particular reference to Vanadium and Titanium"*. HSLA Steels: Processing, Properties and applications, The Metals & Materials Society,1992 p 51-60.
53. W. B. Lee, S. G. Hong, C. G. Park, K. H. Kim and S. H. Park. "*Influence of Mo on Precipitation Hardening in Hot Rolled HSLA Steels Containing Nb*." Scripta Mater. 43(2000) 319-324.
54. E. V. Pereloma, B. R. Crawford, P. D. Hogdson, "Strain induced Precipitation behavior in hot rolled steel", Materials Science and Engineering, A299 (2001) p 27-37.
55. A. Fragiel, R. Schouwenaarf, R. Guardian, R. Perez, "*Microstructural characteristics of different commercially available API X65 steels*" ,Journal of new materials for electrochemical systems 8, 115-119 (2005).

56. E. S. Davenport, E. C. Bain. "*Transformation of austenite at constant subcritical temperatures*", Transactions AIME, Vol 90, 1930, p 117–144; reprinted as a Metallurgical Classic, with commentary by Harold W. Paxton, in Metallurgical Transactions, Vol. 1, (1970), pp. 3475–353.
57. W. T. Reynolds, H. I. Aaronson, G. Spinose, "*A summary of the present diffusionist views on bainite*, *Materials Transactions*", JIM, Vol 32, No. 8, (1991), pp. 737–746.
58. Y. E. Smith, A. P. Coldren, R. L. Cryderman. "*Toward improved ductility and toughness*", Climax Molybdenum Company Ltd. (1972), pp. 119–142.
59. G. I. Rees, H. K. D. H. Bhadeshia. "*Thermodynamics of acicular ferrite nucleation*", Mater. Sci. Technol. Vol 10, (1994) pp. 353–358.
60. S. H. Hashemi, D. Mohammadyani, M. Pournvari, S.M.Mousavizadeh. Fatigue Fracture.Eng. Mats.Struct.32 (2009) 33-40.
61. J. S. Lee, J. B. Lu, J. I. Jang, W. S. Kim, D. Kwon, Mater sci.Eng A373 (2004) 122-130.
62. API 1104 "*Standard for welding pipelines and related facilities*", American petroleum institute: 49 CFR 195.214 (a) 19th edition, September 1999.
63. DNV-OS-F101 "*Off shore standard for submarine pipeline systems*" Det Norske Veritas, August 2012.
64. J. B. Lu, W. S. Kim, J. I. Jang, "*Variation in DBTT and CTOD with in weld heat affected zone in API X65 pipe steel*", Materials Science and Engineering A 546 (2012) 258– 262.
65. R. V. B. Gomes, C. H. Aidar, S. S. Kojima, "*Study of fracture mechanics in API X65 and X70 steel pipes*".